ELSEVIER

Surface and Coatings Technology 74–75 (1995) 890–896

SURFACE & COATINGS TECHNOLOGY

Structure and electron emission characteristics of sputtered lanthanum hexaboride films

W. Waldhauser [a], C. Mitterer [a], J. Laimer [b], H. Störi [b]

[a] *Institut für Metallkunde und Werkstoffprüfung, Montanuniversität, Franz-Josef-Straße 18, A–8700 Leoben, Austria*
[b] *Institut für Allgemeine Physik, Technische Universität, Wiedner Hauptstraße 8–10, A–1040 Wien, Austria*

Abstract

Thermionic coatings of lanthanum boride were deposited onto molybdenum and tungsten substrates employing d.c. magnetron sputtering from LaB_6 targets. The influence of the deposition parameters on the structure and the morphology was investigated by means of scanning electron microscopy and X-ray diffraction. The work function and electron emission characteristics of the coatings have been studied by the thermionic emission method using coated tungsten filaments. After optimization of the sputtering parameters, argon pressure, substrate bias voltage and sputtering power density, extremely fine-columnar coatings consisting of predominantly (100)-oriented La–B crystals were obtained. The work function was measured to be approximately 2.8 eV. LaB_6-coated hairpin cathodes worked with comparable electron emission current at temperatures approximately 1000 °C below the operating temperature of uncoated tungsten filaments.

Keywords: Electron emission; Thermionic coatings; Lanthanum hexaboride; Physical vapour deposition; Magnetron sputtering

1. Introduction

The hexaborides of the rare earth and alkaline earth elements are known as excellent thermionic emitters [1]. Among the many hexaborides available lanthanum hexaboride (LaB_6) seems to be the most promising electron emissive material [2] which combines properties such as a low work function with values from 2.4 eV [3] to 2.9 eV [2], a low resistivity of approximately 30 μΩ cm [1], a high melting point of 2715 °C [3], high chemical stability and low evaporation rates.

At present, either rods of sintered LaB_6 or single LaB_6 crystals are indirectly heated to induce emission, or metal filaments such as tungsten, rhenium or tantalum are electrophoretically coated with LaB_6, annealed (sintered) and directly heated. Representing very good emitters, both types of cathodes are generally fragile and can withstand only a limited number of thermal shocks. In addition, indirectly heated LaB_6 electron sources complicate the design of electron guns and consume more heating power. Single crystals of LaB_6 are rather expensive.

Electrophoretically coated metal filaments being simple in design were described by Favreau [4] and Khairnar et al. [5]. Unfortunately, these deposition methods produce porous coatings with low adhesion [6]. In general, coatings fabricated by physical vapour deposition techniques are more dense, adherent and smoother than coatings deposited by electrophoretic methods. Mroczkowski [6] deposited LaB_6 onto tungsten and rhenium filaments employing r.f. magnetron sputtering and obtained coatings with work function values of 2.4–2.6 eV. Yutani et al. [7] prepared thin films at several substrate temperatures by electron beam evaporation with different angles of incidence of the particle flux and yielded work function values of 2.7–2.8 eV.

In this paper we report on the influence of the deposition parameters on the structure and the morphology of La–B coatings deposited by non-reactive d.c. magnetron sputtering using LaB_6 targets. The electron emission characteristics of the coatings have been investigated by the thermionic emission method.

2. Experimental

The coatings were fabricated by non-reactive d.c. magnetron sputtering in a modified CVC sputtering unit (type AST 601) using a commercially available LaB_6 target (diameter, 75 mm; thickness, 6 mm). Deposition was carried out in the static (substrates without move-

ment) and dynamic (rotating substrates) modes. The substrates used were ground molybdenum and metallographically polished tungsten sheets with thicknesses of 0.5 mm for structural investigations as well as various commercially available tungsten cathodes (filament diameter, 0.1 mm) for thermionic emission measurements. All substrates were precleaned with ethylene in an ultrasonic cleaner and could be either grounded or biased up to −1600 V for sputter cleaning prior to deposition. The deposition temperature was maintained using a resistant heater at 200 °C. The deposition was carried out using argon (purity, 99.999%) at chamber pressures ranging from 1 to 4 Pa. Lower or higher pressures, respectively, resulted in flaky peeling of the coatings. The target–substrate distance was 60 mm for static deposition. The thicknesses of those coatings deposited onto molybdenum and tungsten sheets reached 3 ± 1 μm. The dynamic deposition was carried out onto rotating substrates at a mean target–substrate distance of approximately 62 mm and resulted in coating thicknesses of 1.5–2.5 μm. The film thicknesses and deposition rates were determined using a spherical abrasion method [8,9]. In the case of the filaments the thickness was directly measured from scanning electron microscopy (SEM) fracture cross-sections. Heat treatment up to 900 °C in a resistively heated furnace in argon atmosphere was carried out to investigate the thermal stability of the coatings. Prior to and after annealing the coatings deposited onto tungsten sheets were examined by SEM and X-ray diffraction (XRD) with Cr Kα radiation.

A schematic representation of the diode test cell used for the thermionic electron emission measurements performed is given in Fig. 1. The vacuum chamber used was pumped down to approximately 5×10^{-4} Pa by a turbomolecular pumping unit. The filament was resistively heated to 900–1400 °C. The cathode temperatures were measured by a thermocouple-calibrated optical pyrometer. A tantalum disk biased to +300 V was placed as an electron collector at a distance of 10 mm from the cathode. The guard ring used guaranteed that the collector current measured was emitted from the centre of the filament with uniform temperature. Under these conditions, the measurements were performed in the temperature-limited region. There, the emission current density J is determined by Richardson–Dushman's law

$$J = AT^2 \exp\left(\frac{-e\phi}{kT}\right) \tag{1}$$

where A, T, ϕ, and k are the mean effective Richardson constant, temperature, work function, and Boltzmann constant respectively. According to Eq. (1), a $\ln JT^{-2}$ versus T^{-1} plot gives a straight line and the work function ϕ can be evaluated from its slope.

3. Results and discussion

In agreement with other authors [6,10–12] the argon pressure showed the strongest influence on film structure and properties. Films deposited in the static mode at argon pressures ranging from 2.5 to 3.5 Pa, substrate bias voltages between −50 and −100 V and at a substrate temperature of 200 °C were dense, smooth, adherent and dark violet in colour. Static deposition at a sputtering power density of 4.8 W cm^{-2} resulted in

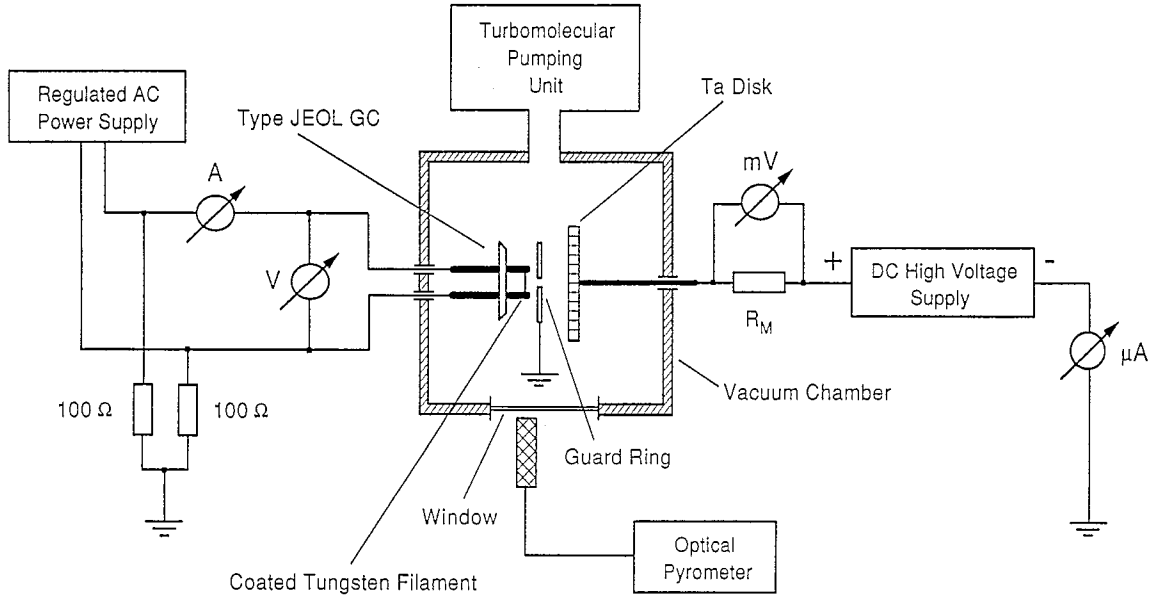

Fig. 1. Simplified schematic diagram of the equipment for electron emission measurements of coated filaments.

growth rates of 40–50 nm min^{-1}. The typical morphology of La–B coatings deposited onto polished tungsten substrates is shown in the SEM micrographs in Fig. 2. Static deposition results in a dense, fracture-amorphous film structure (Fig. 2(b)) with an extremely smooth coating surface (Fig. 2(a)). The variation of the deposition parameters argon flow, bias voltage and substrate temperature indicated that in the case of static deposition the fine-columnar structure is formed at conditions with moderate energetic contribution to the film growth. In the complementary growth region, i.e. extremely low or high energetic contribution, the structure of the coatings becomes fine-grained to fracture-amorphous [12]. On the contrary, coatings deposited onto rotating substrates exhibit generally a fine-columnar structure (Fig. 2(d)) showing a micro-rough and micro-porous surface (Fig. 2(c)). The rotation of the substrates results in a discontinuous flux of sputtered target atoms and argon ions depending on the alignment of the substrate surface to the target. This may cause lower average substrate temperatures hindering diffusion and thus favouring columnar growth [13].

Typical XRD traces of coatings deposited onto tungsten substrates are shown in Fig. 3. In Fig. 3(a), the relative peak heights are given for randomly orientated LaB_6 and tungsten (corresponding to the JCPDS powder diffraction file [14,15]). The intensities have been corrected for the Cr Kα and Cr Kβ radiation [16]. In all films investigated, the formation of the cubic LaB_6 phase exhibiting a distinct (100) texture (Figs. 3(b) and 3(c)) could be detected. However, a significant distinction in the lattice parameters and peak intensities between coatings fabricated by static or dynamic deposition, respectively, was observed. Static deposition at an argon pressure of 3 Pa resulted in XRD peaks of low intensity (Fig. 3(b)) indicating an extremely fine-grained film structure. The lattice parameter a was calculated from the (100) peak as 4.262 Å, corresponding to a distortion of +2.62% with respect to the standard value of LaB_6 (a=4.153 Å [13]). In agreement with Kajiwara et al. [17], the existence of compressive stresses in the films can be concluded. Coatings deposited at corresponding sputtering parameters onto rotating substrates show very sharp and intense peaks (Fig. 3(c)) which are related to the higher crystallinity of these films. The lattice parameter of a=4.197 Å corresponds to a lattice distortion of +1.06%. The differences in the lattice parameter between static and dynamic deposition are interpreted by the possibility of stress relaxation at voided grain boundaries (see Fig. 2) resulting in decreasing distortion.

The texture coefficients $TC_{(hkl)_j}$ [18]

$$TC_{(hkl)_j} = \frac{I_{(hkl)_j}/I_{(hkl)_{j,0}}}{1/n \sum_{i=1}^{n} I_{(hkl)_i}/I_{(hkl)_{i,0}}} \quad (2)$$

where I and I_0 are the intensity values for a peak (hkl) of interest taken from the XRD traces and the powder

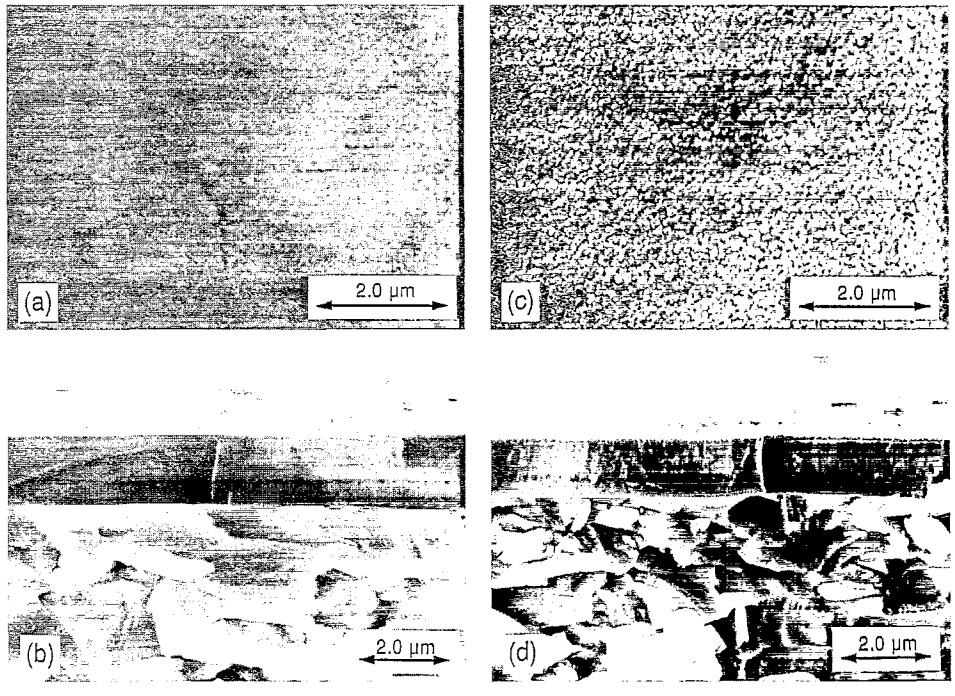

Fig. 2. SEM micrographs of La–B coatings deposited onto polished tungsten sheets. Sputtering power density, 4.8 W cm^{-2}, total pressure, 3.0 Pa; bias voltage, −50 V; substrate temperature, 200 °C. (a) Static deposition without movement of the substrate (surface view); (b) static deposition without movement of the substrate (fracture cross-section); (c) dynamic deposition onto a rotating substrate (surface view); (d) dynamic deposition onto a rotating substrate (fracture cross-section).

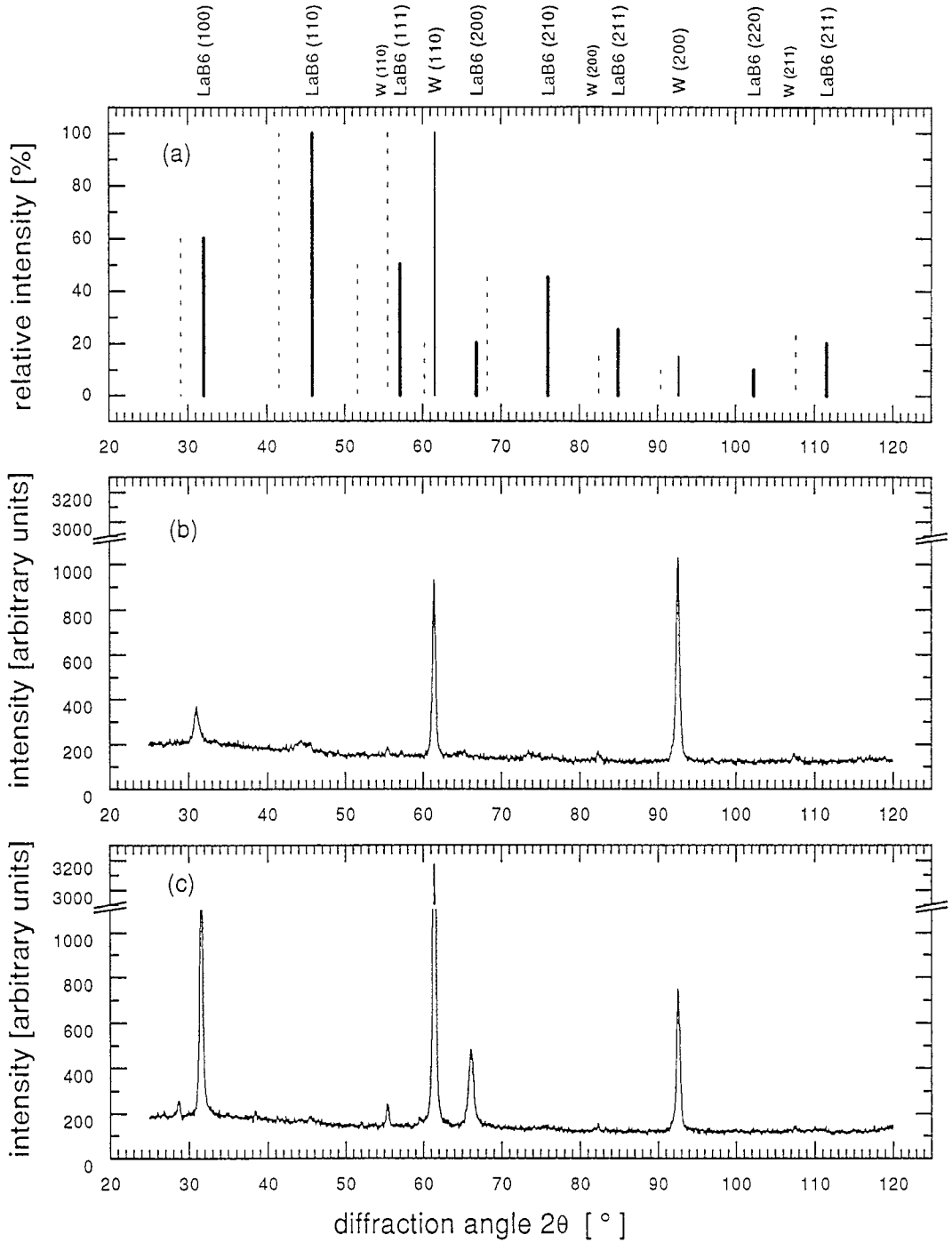

Fig. 3. XRD traces of LaB_6 powder and La–B coatings deposited onto tungsten substrates (Cr Kα radiation). Sputtering power density, 4.8 W cm^{-2}; total pressure, 3.0 Pa; bias voltage, −50 V; substrate temperature, 200 °C. (a) Powder diffraction file [14] (Kα and Kβ peaks); (b) static deposition without movement of the substrate; (c) dynamic deposition onto a rotating substrate.

diffraction file respectively, and n is the number of peaks considered, were calculated for coatings deposited onto molybdenum and tungsten substrates. It should be noted that a random orientation would lead to TC values of unity whereas a complete dominance of one peak would return the number n of peaks considered.

Corresponding to earlier work [11,12] the distinct (100) texture of the LaB_6 phase becomes even more dominant with increasing argon pressure (Fig. 4(a)), whereas the lattice parameters calculated from the diffraction peaks decrease with increasing argon pressure (Fig. 4(b)). This behaviour can be interpreted by the increased number of collisions of the sputtered energetic particles with argon atoms resulting in a larger number

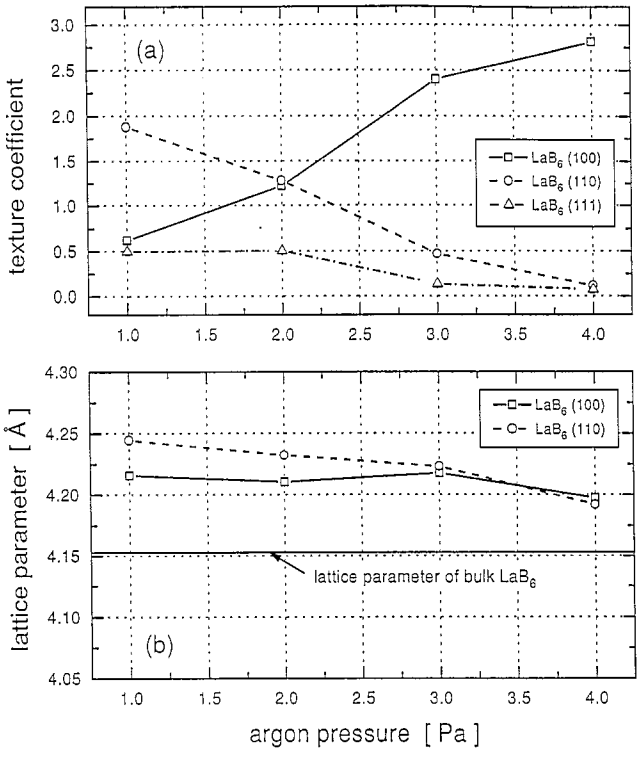

Fig. 4. Texture coefficients (a) and lattice parameters (b) of the LaB_6 phase in coatings deposited onto molybdenum substrates as a function of the argon pressure. Static deposition: sputtering power density, 4.8 W cm^{-2}; bias voltage, −100 V; substrate temperature, 200 °C.

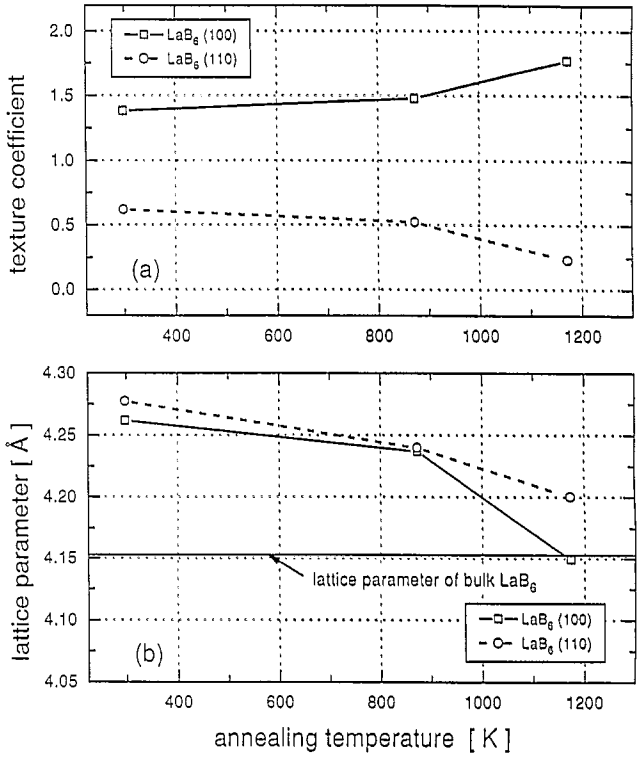

Fig. 5. Texture coefficients (a) and lattice parameters (b) of the LaB_6 phase in coatings deposited onto tungsten substrates as a function of the annealing temperature after deposition. Static deposition: sputtering power density, 4.8 W cm^{-2}; total pressure, 3.0 Pa; bias voltage, −50 V; substrate temperature, 200 °C.

of thermalized atoms [19] and a decreased number of argon atoms incorporated interstitially in the LaB_6 lattice [11,12].

In Figs. 5(a) and 5(b) the dependences of the texture coefficient and lattice parameter of coatings deposited in the static mode onto polished tungsten substrates on the annealing temperature after deposition are shown. As can be seen from Fig. 5(a), the distinct (100) orientation of the LaB_6 phase becomes more dominant with increasing annealing temperature. At the same time the lattice distortion is decreasing with increasing annealing temperature (Fig. 5(b)). Obviously due to thermal stresses coatings with thicknesses of 3 μm tended to flaky peeling after annealing for 30 min at 900 °C during heat treatment or cooling down respectively. In contrast to this, coatings deposited dynamically onto tungsten filaments were adherent throughout emission testing at temperatures of up to 1400 °C. This is attributed on the one hand to the open structure of coatings deposited dynamically (compare Figs. 2(c) and 2(d)) and on the other hand to the relative high ratio between coating and substrate thickness. Both facts allow the relaxation of thermal stresses [20].

Fig. 6 shows the emission current of coated and uncoated tungsten hairpin cathodes as a function of the temperature. Before emission testing the heating current was increased slowly and the cathode surface was activated by maintaining an annealing temperature of the coated filaments of 900 °C for 30 min. It can be seen from Fig. 6 that a coated filament works at temperatures approximately 1000 °C below the operating temperature of an uncoated tungsten filament while emitting the same electron current. The Richardson plot of a coated tungsten cathode with straight filament (Fig. 1) given in Fig. 7 shows a good linearity. The work function was calculated as about 2.8 eV which is in good agreement with values measured by Yutani et al. [7].

Figs. 8(a)–8(c) show the surface and fracture cross-section of a coated cathode with straight filament prior to emission testing. Grooves formed during wire-pulling are reproduced by the coating. The typical film morphology obtained by dynamic deposition with voided grains can be seen clearly (compare Fig. 2(c)). The smooth and well adherent La–B coating shows a small number of surface defects such as droplets (Fig. 8(a)) caused by arcs igniting especially at high bias voltages or low argon pressures when using compound targets with low density [12,21]. Additionally, the periodically varying target–substrate distance during dynamic deposition is suspected to increase the possibility for arc ignition. The SEM micrograph in Fig. 8(c) indicates an inhomogeneous coating thickness distribution caused by shadowing effects during deposition owing to the above-mentioned

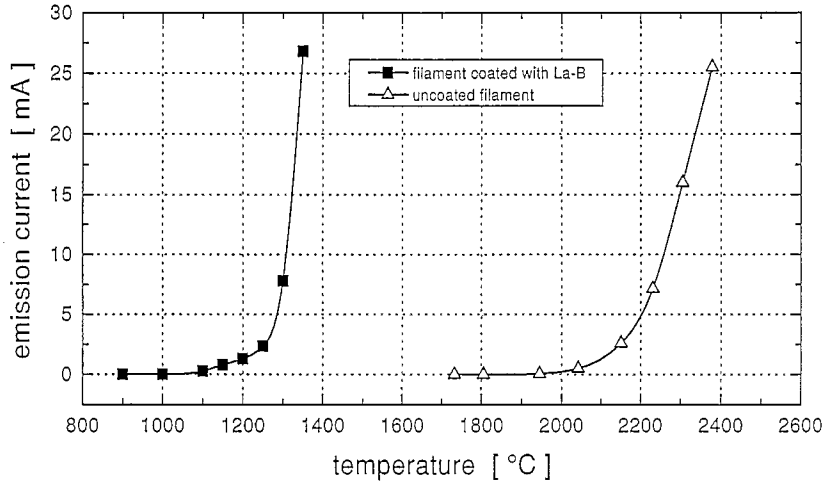

Fig. 6. Emission current of La–B-coated (■) and uncoated (△) tungsten hairpin cathodes as a function of the operating temperature.

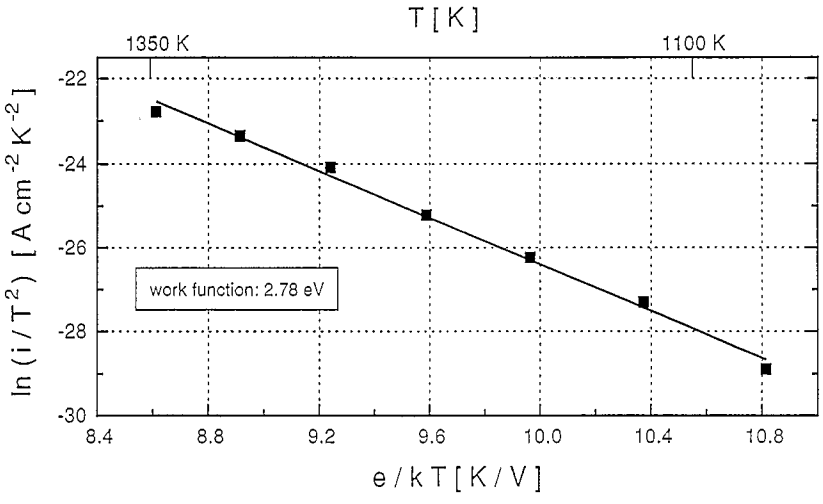

Fig. 7. Richardson plot of a La–B-coated tungsten cathode with straight filament. Dynamic deposition: sputtering power density, 4.8 W cm^{-2}; total pressure, 3.0 Pa; bias voltage, −50 V; substrate temperature, 200 °C.

grooves. After emission testing at temperatures of up to 1400 °C the formation of cracks (Fig. 8(d)) caused by the difference in the thermal coefficient of expansion between the core wire and the coating could be detected. However, no detachment of the coating was observed. Inferred from the work of Khairnar et al. [5], the difference in the thermal coefficient of expansion affects the number of sustainable thermal shocks occurring during normal operation cycles and thus the life time of the cathode. As can be seen from Figs. 8(e) and 8(f), the heat treatment during emission testing leads to the formation of a coarse film structure with decreasing density. This may be caused by recrystallisation, diffusion and evaporation processes occurring at these temperatures. The relative high residual pressure of 5×10^{-4} Pa during emission testing is suspected to influence these processes thus affecting the life time.

4. Conclusions

Extremely fine-columnar films with a predominantly (100)-oriented LaB_6 phase were prepared by magnetron sputtering of LaB_6 targets in static and dynamic modes at argon pressures ranging preferably from 2.5 to 3.5 Pa. The work function of the coatings measured by the thermionic emission method using coated tungsten filaments showed values of 2.8 eV corresponding to the literature. In contrast to bulk LaB_6 cathodes used at present, coated metal filaments seem to be very promising with respect to their simple fabrication, lower operating temperature and thus lower power consumption. However, further investigations are necessary to determine application-related properties, such as current stability, life time and resistance against thermal shocks.

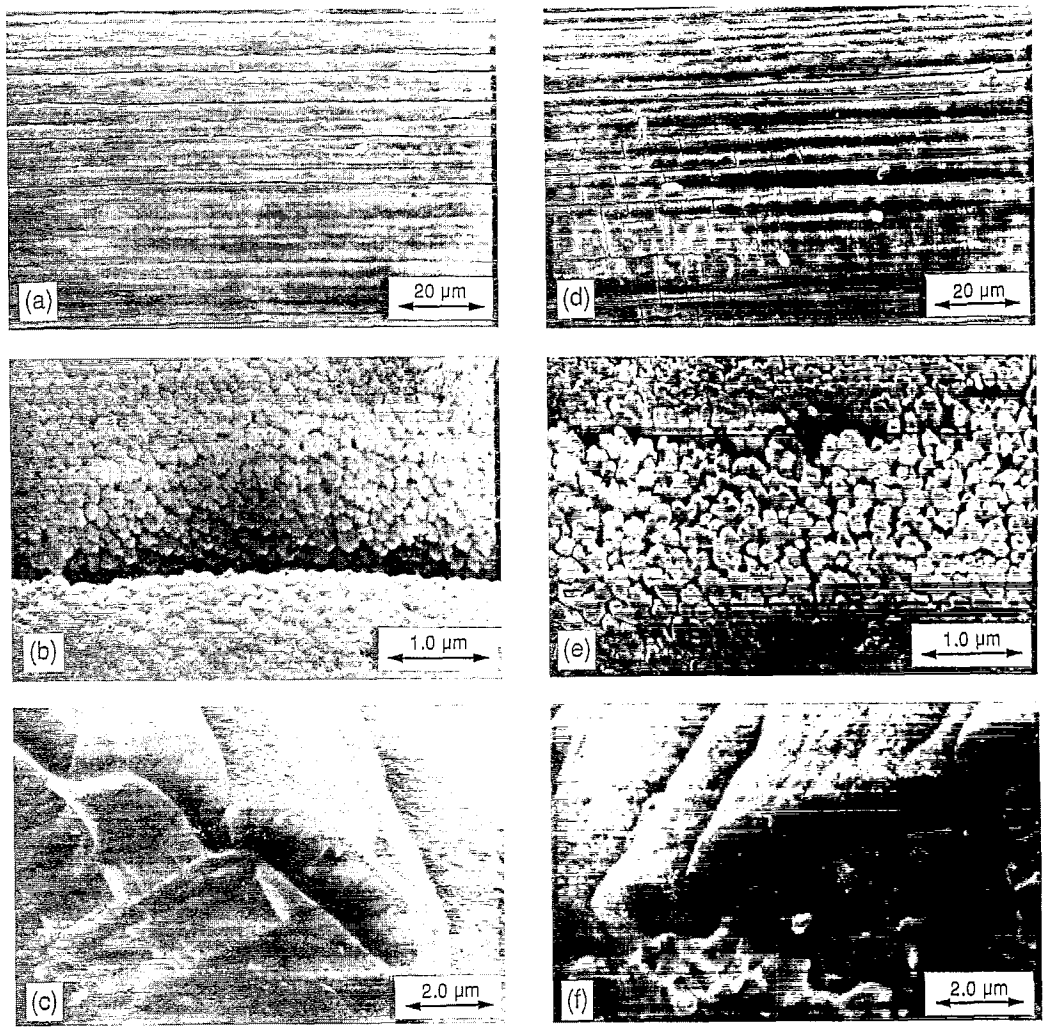

Fig. 8. SEM micrographs of La–B-coated tungsten cathodes with straight filament prior to ((a)–(c)) and after ((d)–(f)) thermionic emission testing at temperatures of up to 1400 °C. Dynamic deposition: sputtering power density, 4.8 W cm^{-2}; total pressure, 3.0 Pa; bias voltage, −50 V; substrate temperature, 200 °C.

Acknowledgement

This work was supported by the Bundesministerium für Wissenschaft und Forschung (Austria).

References

[1] J.M. Lafferty, *J. Appl. Phys., 22* (1951) 299.
[2] M. Futamoto, M. Nakazawa and U. Kawabe, *Surf. Sci., 100* (1980) 470.
[3] F. Binder, *Radex-Rundschau, 4* (1975) 531.
[4] L.J. Favreau, *Rev. Sci. Instrum., 36* (1965) 856.
[5] R.S. Khairnar, P.W. Mahajan, D.S. Joag, A.S. Nigavekar and P.L. Kanitkar, *J. Vac. Sci. Technol., A3*(2) (1985) 398.
[6] S.J. Mroczkowski, *J. Vac. Sci. Technol., A9* (1991) 586.
[7] A. Yutani, A. Kobayashi, A. Kinbara, *Appl. Surf. Sci., 70/71* (1993) 737.
[8] K. Herf and E. Roeder, *Prakt. Metall., 6* (1968) 557.
[9] B. McDonald and A. Goetzberger, *J. Electrochem. Soc., 109* (1962) 141.
[10] W. Waldhauser, C. Mitterer, P. Schmölz, H. Störi and J. Barounig, in H. Bildstein and R. Eck (eds.), *Proc. 13th Int. Plansee Seminar*, Metallwerk Plansee, Reutte, 1993, Vol. 4, p. 267.
[11] J. Stallmaier, C. Mitterer and J. Barounig, Proc. 11th Int. Conf. on Vacuum Metallurgy, *Le Vide, les Couches Minces, 261* (1992) 265.
[12] C. Mitterer, J. Komenda-Stallmaier, P. Losbichler, P. Schmölz and H. Störi, *Surf. Coat. Technol., 74–75* (1995) 1020.
[13] J.A. Thornton, *Ann. Rev. Mater. Sci., 7* (1977) 239.
[14] *Powder Diffraction File, Card 6-0401*, Joint Committee on Powder Diffraction Standards, International Center for Diffraction Data, Swarthmore, PA, 1950.
[15] *Powder Diffraction File, Card 4-0806*, Joint Committee on Powder Diffraction Standards, International Center for Diffraction Data, Swarthmore, PA, 1951.
[16] B.D. Cullity, *Elements of X-ray Diffraction*, Addison-Wesley, Reading, MA, 1978, p. 131.
[17] T. Kajiwara, T. Urakabe, K. Sano, K. Fukuyama, K. Watanabe, S. Baba, T. Nakano and A. Kinbara, *Vacuum, 41*(4–6) (1990) 1224.
[18] A.J. Perry and J. Schoenes, *Vacuum, 36*(1–3) (1986) 149.
[19] R. Elsing, *Surf. Coat. Technol., 49* (1991) 132.
[20] J.-E. Sundgren, *Thin Solid Films, 128* (1985) 21.
[21] P.C. Johnson, in J.L. Vossen and W. Kern (eds.), *Thin Film Processes II*, Academic Press, San Diego, CA, 1991, pp. 242–244.